Fabrication of Sintered Porous Poly(L-lactide) Scaffold with Controlled Pore Size and Porosity

Fumio Teraoka, Masashi Hara, Masafumi Nakagawa, Taiji Sohmura

Division of Biomaterial Science, Graduate School of Dentistry, Osaka University, Osaka, Japan

Received 25 June 2009; accepted 27 December 2009
DOI 10.1002/app.32013
Published online 29 March 2010 in Wiley InterScience (www.interscience.wiley.com).

ABSTRACT: The aim of this study was to control the pore sizes, porosities, and mechanical properties of three-dimensional scaffolds by varying the particle sizes, sintering temperature, and sintering time. The surface and inner morphologies of the scaffolds were evaluated using a scanning electron microscope and an X-ray microfocus CT, respectively. Furthermore, the mechanical properties of the scaffold were discussed. The sintered scaffolds had a total porosity between 15% and 54% with a median pore size in the range of 65–340 μm. By varying the particle sizes and the sintering temperature at a constant sintering time (15 min), the flexural strength and flexural modulus changed from 9.09 ± 1.33 MPa to 44.64 ± 3.31 MPa and from 0.51 ± 0.04 GPa to 1.11 ± 0.09 GPa, respectively. These results indicate that the sintered scaffolds are suitable for bone tissue engineering as load-bearing scaffolds. © 2010 Wiley Periodicals, Inc. J Appl Polym Sci 117: 1566–1571, 2010

Key words: poly(L-lactide) (PLLA); sintering; porous scaffold; pore size; strength

INTRODUCTION

A small damaged part of bone naturally regrows by healing. However, if large volumes of tissue over a critical amount are removed, the body is not able to completely regenerate an entire new piece of bone. In these cases, an artificial scaffold is needed for regeneration by tissue engineering. Generally, bioceramics or biodegradable polymers are used for the artificial scaffold.[1–3] The materials used for fabricating scaffolds for bone tissue engineering applications should have a mechanical strength sufficient enough for bone cells to attach and proliferate.

Bioceramics, such as hydroxyapatite (HAp)[4–8] and tricalcium phosphate (TCP),[9] are widely used as scaffold materials for bone regeneration due to their excellent biocompatibility, osteoconductivity, biodegradability, and mechanical strength. Though they are difficult to process because of their material properties,[4,5] some studies have reported new fabrication methods of hydroxyapatite scaffold.[10]

Many synthetic biodegradable polymers, such as poly(L-lactide) (PLLA),[11] polyglycolic acid (PGA), polycaprolactone (PCL)[12] and their copolymers, are extensively used as artificial scaffolds. These polymers have superior characteristics for easily making porous scaffolds. A number of processing techniques based on solvent casting and particulate-leaching,[13] extrusion, gas foaming, freeze drying,[14] phase separation, textile technologies, particle aggregation,[15] and solid freeform fabrication[16] have already been developed to produce porous biodegradable polymeric scaffolds for tissue engineering applications. Of these methods, the solvent casting and particulate-leaching, extrusion, gas foaming, freeze drying and phase separation methods involve toxic solvents and incomplete removal of residual particulates from the polymer. Furthermore, when using these methods, it is difficult to control the pore size, porosity and shape, and to create interconnections within the scaffold for vascularization. The use of a sintering process for the polymer particles will circumvent such limitations.

In this study, we fabricated PLLA porous scaffolds using the sintering method. Varying the particle size, sintering temperature and sintering time controlled the pore size, porosity, and the mechanical properties. Scanning electron microscopy (SEM) and X-ray microfocus CT were used to characterize the morphologies and microstructures of the PLLA fabricated scaffolds.

MATERIALS AND METHODS

Scaffold preparation

Poly(L-lactide) (PLLA) with an average molecular weight (Mw) of 220,000 g/mol and the polydispersity (Mw/Mn) of 2.3 was obtained from a commercial source (Lacty 5000, Shimazu, Kyoto, Japan) in

Correspondence to: F. Teraoka (terachan@dent.osaka-u.ac.jp).

pellet form. The pellets were crushed after freezing under liquid nitrogen, and then particles of 75, 125, 250, and 350 μm average sizes were adjusted by using sieves. The 3D scaffolds were fabricated by packing the particles into a stainless steel mold. The mold was heated to different sintering temperatures (160, 170, 180, and 190°C) for different sintering times (10, 15, and 30 min). The mold was then allowed to cool to room temperature) (25°C) before the samples were removed. Finally, the samples (PLLA disks of 15 mm diameter × 6 mm thickness) were removed from the mold and stored under vacuum until used. The sintered scaffolds with the particles of 75, 125, 250, and 350 μm were labeled PLLA-75, PLLA-125, PLLA-250, and PLLA-350, respectively.

Differential scanning calorimetry (DSC)

A thermal analysis was performed by a differential scanning calorimeter (DSC-60, Shimadzu, Kyoto, Japan) using 10 mg of the particles crushed after freezing at the heating rate of 10°C/min from 40 to 220°C. The experiment was carried out in a nitrogen atmosphere.

Scanning electron microscopy (SEM) and X-ray microfocus CT

The surface of the scaffolds were coated with gold and observed using a scanning electron microscope (VE-7800, Keyence, Osaka, Japan) at the accelerating voltage of 20 kV.

The inner morphology of the scaffolds was observed using an X-ray microfocus CT (TDM-1000, Yamato, Tokyo, Japan) with a tube voltage of 90 kV and a tube current of 0.010 mA. A voxel size of 21.48 μm was selected and the reconstruction image matrix size was 512 × 512 × 512. A schematic diagram of the sample and shooting dimensions of the X-ray-CT are shown in Figure 1. The *X-Y* plane, and the *X-Z* and *Y-Z* planes show the cross section in parallel to the surface and in perpendicular to the surface, respectively.

Pore size and porosity

The total porosity and median pore size of the scaffolds were measured using a mercury intrusion porosimeter (Micromeritics Automated Mercury Porosimeter IV 9505, Shimadzu, Kyoto, Japan). The partial porosity in each cross-sectional area of the scaffold was estimated using the image analysis (NIH Image, MD, USA) from the X-ray microfocus CT image. Briefly, the porosity was calculated from the proportion of the area of pores divided by the total cross sectional area to the total cross-sectional area.

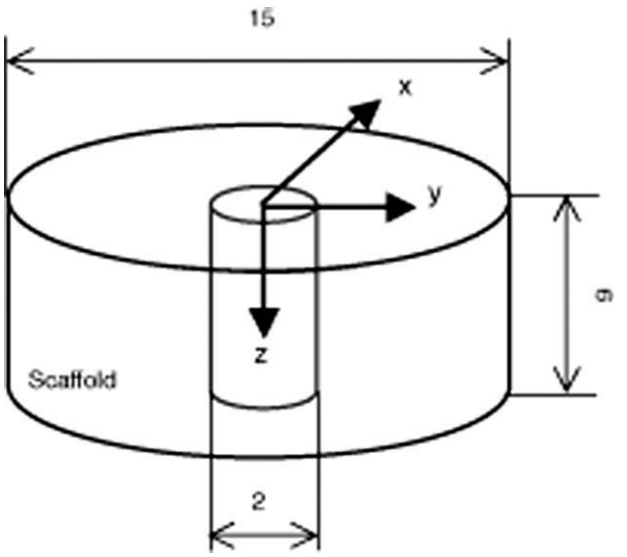

Figure 1 Schematic diagram of scaffold (φ15 × 6 mm) and shooting dimensions (φ2 × 6 mm) of X-ray-CT.

Mechanical properties

The flexural specimens (10 × 60 × 3 mm^3) were directly obtained by sintering in the mold. The flexural tests were performed using a universal testing machine (EZ-Test, Shimadzu, Kyoto, Japan) in a three-point bending mode on five specimens. The span length and crosshead speed were 30 mm and 1 mm/min, respectively.

The compressive specimens (5 mm diameter and 10 mm thickness to produce a 2 : 1 aspect ratio) were cut from the sintered specimens (30 × 30 × 10 mm^3). Compressive tests were performed using the universal testing machine at the crosshead speed of 1 mm/min on five specimens.

All tests were conducted in the laboratory at room temperature (23 ± 3°C and 50 ± 5% relative humidity).

Statistical analysis

The mean value and the standard deviation of the obtained data were calculated, and the significance test was done using the two way analysis of variance (ANOVA) and post hoc tests. They were then statistically analyzed to a significance level of 5% using the Fisher's multiple comparison tests. The different letters in the figure indicate that there was a significant difference.

RESULTS AND DISCUSSION

The PLLA crushed after freezing was a semi-crystalline polymer that had a glass transition temperature of 56°C and a melting temperature of about 160°C (Fig. 2). On the basis of the DSC data, we

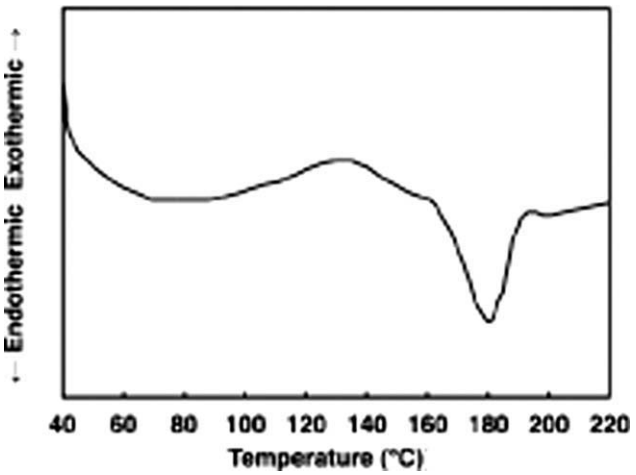

Figure 2 DSC curve of the PLLA crushed after freezing.

determined the sintering temperature to be between 160 and 190°C, and the sintering time between 10 and 30 min. Table I shows forming quality of 48 different samples that were sintered using four different particle size under four different temperatures in three different times. A circle shows that all samples were able to be removed in complete shape from the mold after sintering. A triangle shows that most samples were not able to be removed in complete shape from the mold after sintering. A cross shows that most samples were deformed from original shape after sintering. Because all the samples sintered at each temperature for 15 min remained intact after demolding, we experimented using these samples.

The morphology of the fabricated PLLA-250 scaffolds sintered at different temperatures for 15 min are shown in Figure 3. The SEM images showed interconnected porous structures generated by the sintering process. The particles of the PLLA-250 sintered at 160°C were only slightly fused to each other as shown in Figure 3(a). Therefore, the PLLA-250 sintered at 160°C had inferior mechanical properties. The particles of the PLLA-250 sintered at 170°C had a smooth surface, and were partially fused to each other in a small area [Fig. 3(b)]. By increasing the sintering temperature, the fusion among the particles was progressively better [Fig. 3(c)]. On the other hand, in the case of the PLLA-250 sintered at 190°C, the particles were fairly fused and had not maintained their original shape [Fig. 3(d)]. The excessive interconnection among the pores was observed in the SEM image.

The two-dimensional CT-cross sections of the sintered scaffolds are shown in Figure 4. The scaffolds of Figure 4(a,d,g), and Figure 4(b,e,h) are the same samples in Figure 3(b,c), respectively. Then, Figure 4(c,f,i) show the PLLA-125 sintered at 170°C. These scaffolds each had different pore sizes, porosities, and superior interconnections among the pores. No morphological differences between the upper parts [Fig. 4(a–c)] and middle parts [Figs. 4(d–f)] were observed in the CT horizontal cross sections of these scaffolds. The same held true for the vertical cross sections [Figs. 4(g–i)] of these scaffolds. These results suggested that the scaffolds were formed by pressureless sintering.

Figure 5(a) shows the relationship between the pore size and particle size of the scaffolds sintered at 170°C and 180°C for 15 min. When the particle size increased from 75 μm to 350 μm, the median pore size significantly increased from 65.21 ± 4.42 μm to 293.78 ± 16.13 μm (sintered at 170°C), and from 95.03 ± 5.67 μm to 340.66 ± 25.79 μm (sintered at 180°C). Similarly, an increase in the particle size led to a significant increase in the porosity of the scaffolds from 26.23 ± 3.42% to 53.66 ± 5.63% (sintered at 170°C), and from 15.31 ± 2.67% to 41.12 ± 3.69% (sintered at 180°C) [Fig. 5(b)].

The flexural strength and modulus, and compressive strength and modulus of the scaffolds fabricated at different temperatures and different times are shown in Figures 6 and 7, respectively. By increasing the particle size from 75 μm to 350 μm, the flexural strength and modulus significantly decreased from 27.01 ± 2.42 MPa to 9.09 ± 1.33 MPa and from

TABLE I
Forming Quality of 48 Different Samples

	Sintering temperature (°C)											
	160			170			180			190		
	Sintering time (min)											
Sintered scaffolds	10	15	30	10	15	30	10	15	30	10	15	30
PLLA-75	○	○	○	○	○	×	○	○	×	×	×	×
PLLA-125	△	○	○	○	○	○	○	○	×	○	×	×
PLLA-250	△	○	○	△	○	○	○	○	○	○	○	×
PLLA-350	△	○	○	△	○	○	△	○	○	○	○	×

A circle (○) shows that all samples were able to taken out in complete shape from the mold after sintering.
A triangle (△) shows that some samples were not able to taken out in complete shape from the mold after sintering.
A cross (×) shows that some samples were distorted in the mold after sintering.

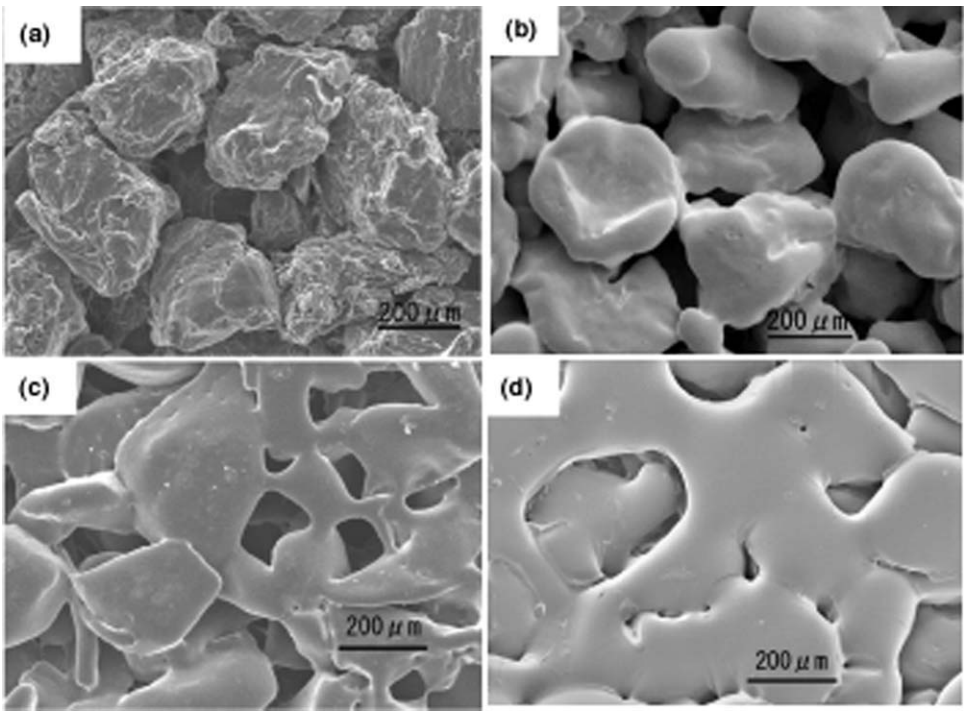

Figure 3 SEM images of PLLA-250 sintered at (a) 160°C, (b) 170°C, (c) 180°C, and (d) 190°C.

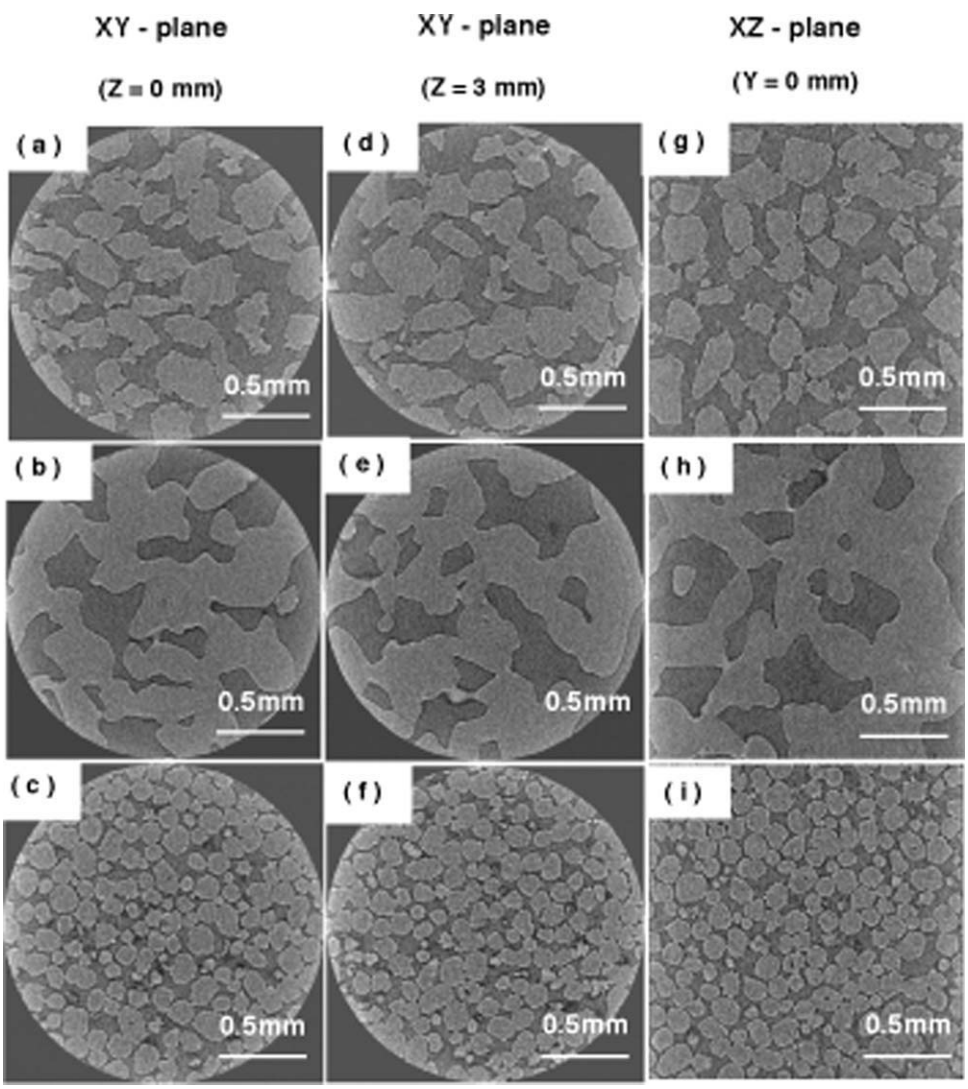

Figure 4 X-ray microfocus CT images of sintered PLLA scaffolds (a), (d) and (g); PLLA-250 sintered at 170°C (b), (e) and (h); PLLA-250 sintered at 180°C (c), (f) and (i); PLLA-125 sintered at 170°C.

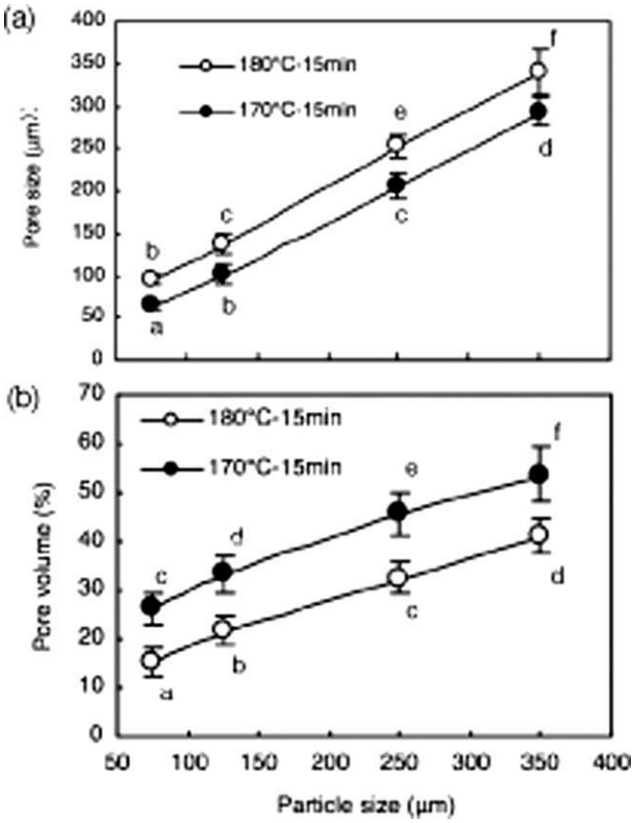

Figure 5 Relationship between pore size (a), porosity (b) and particle size when sintered at 170°C and 180°C for 15 min; where different letter indicates significant difference ($P < 0.05$).

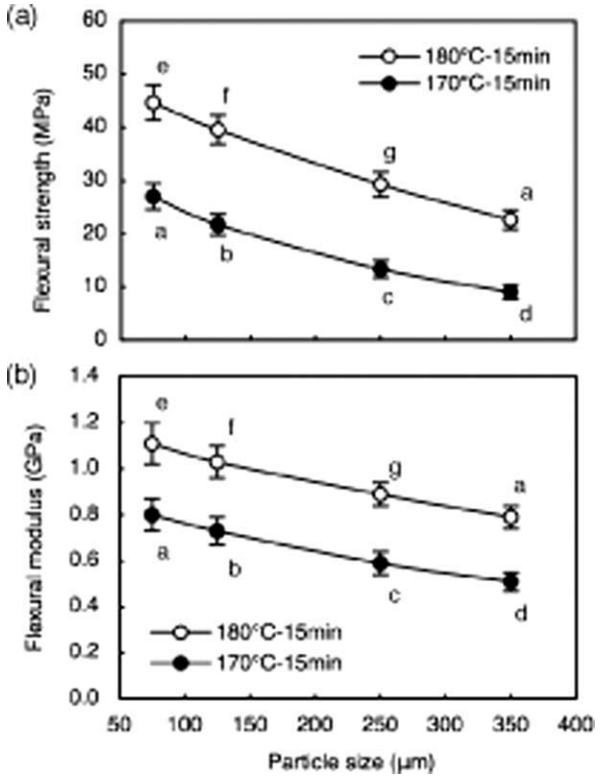

Figure 6 Flexural (a) strength and (b) modulus of PLLA scaffolds sintered at 170°C and 180°C for 15 min; where different letter indicates significant difference ($P < 0.05$).

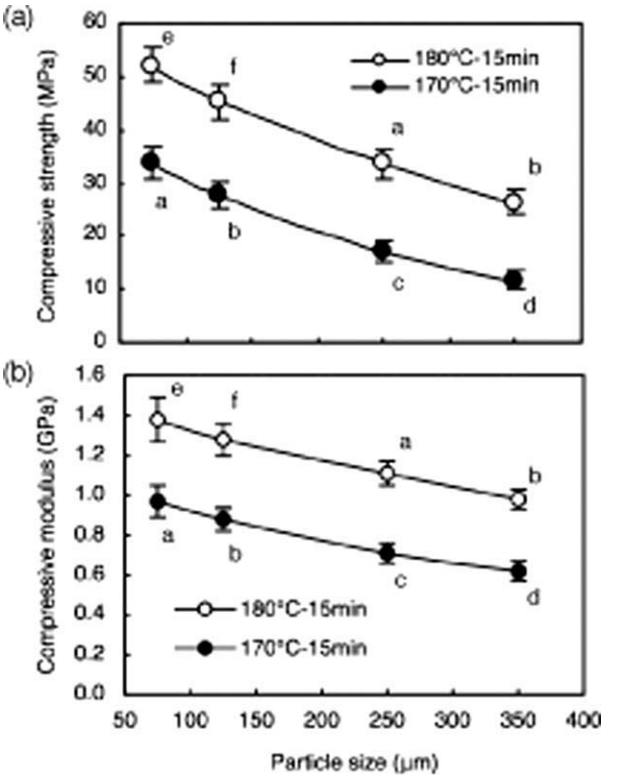

Figure 7 Compressive (a) strength and (b) modulus of PLLA scaffolds sintered at 170°C and 180°C for 15 min; where different letter indicates significant difference ($P < 0.05$).

0.80 ± 0.07 GPa to 0.51 ± 0.04 GPa (sintered at 170°C), and from 44.64 ± 3.31 MPa to 22.62 ± 1.82 MPa and from 1.11 ± 0.09 GPa to 0.79 ± 0.05 GPa (sintered at 180°C), respectively. Similarly, the compressive strength and modulus of the scaffolds significantly decreased from 33.77 ± 3.12 MPa to 11.83 ± 1.93 MPa and from 0.97 ± 0.08 GPa to 0.62 ± 0.05 GPa (sintered at 170°C), and from 52.15 ± 3.38 MPa to 26.38 ± 2.22 MPa and from 1.38 ± 0.11 GPa to 0.98 ± 0.05 GPa (sintered at 180°C), respectively.

Increasing the particle size caused a linear increase in the pore size and porosity at the sintering temperatures of both 170°C and 180°C (Fig. 5). In contrast, the increase in the particle size resulted in a significant decrease in the mechanical properties of the scaffolds (Figs. 6 and 7). These results indicate that the mechanical properties had a close relation to the pore size or porosity. Increasing the sintering temperature increases the area of contact points between the particles (Figs. 3 and 4) and thus increases the mechanical properties of the scaffolds (Figs. 6 and 7). By varying the particle sizes and sintering temperature at a constant sintering time, one could accurately control the pore sizes, porosities, and mechanical properties of the 3D scaffolds. Many

researchers demonstrated that scaffolds with pore sizes in the range of 100–250 μm or larger are suitable for bone regeneration.[1–3] The sintered PLLA scaffolds had median pore sizes in the range of 65–340 μm, which makes them suitable as tissue engineering scaffolds.

The sintered scaffold had many superior characteristics such as being solvent free, complete interconnection of cell structures (Figs. 3 and 4), and high mechanical properties (Figs. 6 and 7). The pore structure in the scaffolds prepared by polymer sintering is characterized by the interconnection of the particles. The scaffold for bone regeneration should have a sufficient structural integrity matching the mechanical properties of native bone tissue. The compressive strength of the sintered scaffolds was the same or greater than that of cancellous bone,[17,18] however, less than one third of the cortical bone.[19] Because of the specific pore structure and superior mechanical properties, the polymer sintered scaffolds will be particularly suitable for load bearing applications such as bone regeneration.

CONCLUSIONS

The purpose of this study was to control pore sizes, porosities, and mechanical properties of the 3D scaffolds by varying the particle sizes, sintering temperature, and sintering time. The sintered PLLA scaffolds have median pore sizes in the range of 65–340 μm. The sintered scaffolds have a compressive strength of the same or greater than that of cancellous bone. These results suggested that the polymer sintered scaffolds are quite suitable for load bearing applications such as bone regeneration.

References

1. Borden, M.; El-Amin, S. F.; Attawia, M.; Laurencin, C. T. Biomaterials 2003, 24, 597.
2. Burg, K. J. L.; Porter, S.; Kellam, J. F. Biomaterials 2000, 21, 2347.
3. Yang, S.; Leong, K. F.; Du, Z.; Chua, C. K. Tissue Eng 2001, 7, 679.
4. Rodríguez-Lorenzo, L. M.; Vallet-Regí, M.; Ferreira, J. M. F. J Biomed Mater Res 2002, 60, 232.
5. Roy, T. D.; Simon, J. L.; Ricci, J. L.; Rekow, E. D.; Thompson, V. P.; Parsons, L. R. J Biomed Mater Res A 2003, 67, 1228.
6. Almirall, A.; Larrecq, G.; Delgado, J. A.; Martínez, S.; Planell, J. A.; Ginebra, M. P. Biomaterials 2004, 25, 3671.
7. Ben-Nissan, B.; Milev, A.; Vago, R. Biomaterials 2004, 25, 4971.
8. Gu, Y. W.; Khor, K. A.; Cheang, P. Biomaterials 2004, 25, 4127.
9. Miranda, P.; Saiz, E.; Gryn, K.; Antoni, P.; Tomsia, A. P. Acta Biomater 2006, 2, 457.
10. Tanimoto, Y.; Hayakawa, T.; Nemoto, K. Dent Mater 2007, 23, 549.
11. Nakagawa, M.; Teraoka, F.; Fujimoto, S.; Hamada, Y.; Kibayashi, H.; Takahashi, J. J Biomed Mater Res A 2006, 77, 112.
12. Tay, B. Y.; Zhang, X.; Myint, M. H.; Ng, F. L.; Chandrasekaran, M.; Tan, L. K. A. J Mater Process Tech 2007, 182, 117.
13. Reignier, J.; Huneault, M. A. Polymer 2006, 47, 4703.
14. Nakao, H.; Hyon, S. H.; Tsutsumi, S.; Matsumoto, T.; Takahashi, J. Dent Mater J 2003, 22, 262.
15. Jiang, T.; Abdel-Fattah, W. I.; Laurencin, C. T. Biomaterials 2006, 27, 4894.
16. Sachlos, E.; Czernuszka, J. T. Eur Cells Mater 2003, 5, 29.
17. Giesen, E. B. W.; Ding, M.; Dalstra, M.; Eijden, T. M. G. J. J Biomech 2001, 34, 799.
18. Yeni, Y. N.; Fyhrie, D. P. J Biomech 2001, 34, 1649.
19. Seal, B. L.; Otero, T. C.; Panitch, A. Mater Sci Eng R Rep 2001, 34, 47.